PROCEEDINGS OF SCIENCE

Extending Global Fits of 4D Composite Higgs Models with Partially Composite Leptons

Ethan Carragher,[a] **Kenn Shern Goh,**[b,*] **Wei Su,**[c] **Martin White**[b] **and Anthony G. Williams**[b]

[a] *Rudolf Peierls Centre for Theoretical Physics, University of Oxford, Parks Road, Oxford OX1 3PU, United Kingdom*

[b] *ARC Centre of Excellence for Dark Matter Particle Physics, Department of Physics, University of Adelaide, South Australia 5005, Australia*

[c] *School of Science, Shenzhen Campus of Sun Yat-sen University, No. 66, Gongchang Road, Guangming District, Shenzhen, Guangdong 518107, P.R. China*

E-mail: ethan.carragher@physics.ox.ac.uk, kennshern.goh@adelaide.edu.au, suwei26@mail.sysu.edu.cn, martin.white@adelaide.edu.au, anthony.williams@adelaide.edu.au,

We perform the first convergent Bayesian global fits of 4D Composite Higgs Models with partially-composite third generation quarks and leptons based on the minimal $SO(5) \to SO(4)$ symmetry breaking pattern. We consider two models with the τ lepton and its associated neutrino in different representations of $SO(5)$. Fitting each model with a wide array of experimental constraints allows us to analyse the Bayesian evidence and currently-observed fine-tuning of each model by calculating the Kullback-Leibler divergence between their respective priors and posteriors. Notably both models are found to be capable of satisfying all constraints simultaneously at the 3σ level at scales of < 5 TeV. From a Bayesian viewpoint of naturalness the model with leptons in the **14** and **10** representations is preferred over those in the **5** representation due to its lower fine-tuning. Finally, we consider the experimental signatures for the preferred parameters in these models, including lepton partner decay signatures and gluon-fusion produced Higgs signal strengths, and discuss their potential phenomenology at future high-luminosity LHC runs.

The XVIth Quark Confinement and the Hadron Spectrum Conference (QCHSC24)
19-24 August, 2024
Cairns Convention Centre, Cairns, Queensland, Australia

*Speaker

 ISSN 1824-8039 . Published by SISSA Medialab.

PoS(QCHSC24)238

1. Introduction

The hierarchy problem—the question of why the Higgs boson mass is much lower than high-energy scales—motivates Composite Higgs Models (CHMs), where the Higgs emerges as a bound state from a strongly-interacting sector at the few-TeV scale, thereby protecting it from large mass corrections [1–3]. In minimal CHMs, the Higgs doublet's four degrees of freedom arise as pseudo-Nambu–Goldstone bosons from the breaking $SO(5) \to SO(4)$ [4, 5], and Standard Model fields are partially composite, with heavier particles coupling more strongly to the composite sector [6].

Early studies focused on the partially composite top and bottom quarks and showed that the embedding of their partners in various $SO(5)$ representations (e.g. **5**, **10**, or **14**) substantially impacts the fine-tuning required for electroweak symmetry breaking [7, 8]. Notably, the M4DCHM^{5-5-5} model, which embeds all composite quark partners in the **5**, predicts realistic $H \to \gamma\gamma$ signal strengths despite its inherent double tuning [9, 10].

In this contribution, we present work that has extended this analysis by incorporating the partial compositeness of third-generation leptons (the τ lepton and its neutrino) [11]. We study two scenarios: one where the lepton partners are embedded in the **5** (LM4DCHM$^{5-5-5}_{5-5}$) and another where the left-handed doublet is embedded in the **14** and the right-handed τ in the **10** (LM4DCHM$^{5-5-5}_{14-10}$) [12]. Global fits are performed using the PolyChord nested sampling algorithm [13, 14], incorporating constraints from SM masses, electroweak precision tests, Z decay ratios, Higgs signal strengths, and bounds on the masses of both quark and lepton partners.

Our Bayesian approach quantifies fine-tuning via the Kullback-Leibler divergence between the prior and posterior distributions. The analysis indicates that including partially composite leptons—particularly with the **14** embedding—can significantly reduce overall fine-tuning, thereby providing a more natural resolution to the hierarchy problem.

2. Model overview

The models considered here are two-site leptonic Minimal 4D Composite Higgs Models (M4DCHMs). In these models, the first site contains the elementary fields (with the same quantum numbers as the Standard Model fields except for the Higgs), while the second site hosts the composite fields together with the Higgs. Each site is governed by its own

$$G \equiv SU(3)_C \times SO(5) \times U(1)_X,$$

and the spontaneous breaking of the overall product group $G^1 \times G^2$ to its diagonal subgroup G^{1+2} produces Goldstone bosons Ω_i that link the two sites. An additional breaking $SO(5) \to SO(4)$ yields pseudo-Nambu–Goldstone bosons (pNGBs) that are identified as the Higgs doublet. The effective decay constant f is related to the decay constants f_1 and f_2 via

$$\frac{1}{f^2} = \frac{1}{f_1^2} + \frac{1}{f_2^2},$$

and is connected to the Higgs vacuum expectation value by

$$f = \frac{v}{s_{\langle h \rangle}},$$

with $v = 246\,\text{GeV}$ and $s_{\langle h \rangle}$ denoting the vacuum misalignment.

2.1 Boson sector

In the boson sector, the Lagrangian comprises the kinetic terms for both the elementary gauge fields (of $SU(3)_C \times SU(2)_L \times U(1)_Y$) and the composite gauge fields (of $SU(3)_C \times SO(5) \times U(1)_X$), along with contributions from the Goldstone boson matrices Ω_i. These matrices parameterize the symmetry breakings, and their associated decay constants f_i determine the breaking scales. The composite sector introduces massive vector bosons, including ten states from $SO(5)$, eight heavy gluons from $SU(3)_C$, and one massive $U(1)_X$ resonance.

2.2 Fermion sector

For the fermion sector, we denote the models by LM4DCHM$^{q-t-b}_{\ell-\tau}$. The quark partners are fixed to be in the fundamental **5** representation of $SO(5)$ for both models whilst lepton partners have two distinct embeddings. In the LM4DCHM$^{5-5-5}_{5-5}$ model, both the left-handed lepton doublet and the right-handed τ are embedded in the **5** representation; whilst the LM4DCHM$^{5-5-5}_{14-10}$ model places the left-handed lepton doublet in the **14** and the right-handed τ in the **10**. The corresponding fermionic Lagrangians contain standard kinetic terms for the elementary and composite fields, mixing terms via link fields such as Ω_1, and Yukawa-like interactions that generate masses after symmetry breaking.

2.3 Higgs potential

The Higgs potential is derived from the low-energy effective fermionic Lagrangian obtained by integrating out the heavy composite fermions. This yields an effective Lagrangian expressed in terms of model-dependent form factors $\Pi_\psi(p^2)$ and $M_\psi(p^2)$ for each fermion species. The fermionic contribution to the potential is given by an integral over Euclidean momentum of a logarithmic function involving these form factors. Gauge boson contributions to the quadratic term in the potential are calculated analytically to first order in $t_\theta := g_0/g_\rho$. Composite gauge boson masses are defined in terms of the decay constants f_1 and f_2.

Our new Higgs mass is then $m_H := \sqrt{8\beta(1-s^2_{\langle h\rangle})}\frac{s_{\langle h\rangle}}{f}$, where β^4 is the quartic coefficient of the expansion of the Higgs potential after expanding it in terms of $s_h := \sin(h/f)$.

3. Scanning Method

3.1 Scan algorithm

In our analysis, we perform global scans over the model parameter space using the nested sampling algorithm `PolyChord` [13]. This method enables comprehensive exploration of the multi-dimensional parameter space and the identification of potential multi-modal posterior distributions. Each parameter point $\mathbf{p}$ is assigned a likelihood, i.e. $\mathcal{L}(\mathbf{p}) = e^{-\frac{1}{2}\chi^2(\mathbf{p})}$, with the total chi-squared $\chi^2(\mathbf{p})$ constructed from contributions of both uncorrelated and correlated observables. For correlated observables, the χ^2 is calculated using the covariance matrix C.

The posterior distribution is obtained via Bayes' theorem:

$$P(\mathbf{p}|\mathcal{M}) = \frac{\mathcal{L}(\mathbf{p})\pi(\mathbf{p}|\mathcal{M})}{Z(\mathcal{M})},$$

where the Bayesian evidence

$$Z(\mathcal{M}) = \int d\mathbf{p}\, \mathcal{L}(\mathbf{p})\pi(\mathbf{p}|\mathcal{M})$$

quantifies the model's overall favourability by balancing the goodness-of-fit with naturalness. In fact, the relation

$$\ln Z = \langle \ln \mathcal{L} \rangle_P - D_{KL},$$

shows that the evidence is determined by the average log-likelihood and the Kullback-Leibler divergence D_{KL}, which measures the difference between the posterior and the prior (and thus the degree of fine-tuning).

`PolyChord` approximates $Z(\mathcal{M})$ via a Riemann sum over the live points. Convergence is achieved when the remaining posterior mass $Z_{\text{live}} \approx X_i \langle \mathcal{L} \rangle_{\text{live}}$ falls below 10^{-3} of the total accumulated evidence.

3.2 Scan parameters

LM4DCHM	**5 – 5**	**14 – 10**
Decay constants	f, f_1, f_X, f_G	f, f_1, f_X, f_G
Gauge couplings	g_ρ, g_X, g_G	g_ρ, g_X, g_G
Quark link couplings	$\Delta_{t_L}, \Delta_{t_R}, \Delta_{b_L}, \Delta_{b_R}$	$\Delta_{t_L}, \Delta_{t_R}, \Delta_{b_L}, \Delta_{b_R}$
Quark on-diagonal masses	$m_t, m_{\tilde{t}}, m_b, m_{\tilde{b}}$	$m_t, m_{\tilde{t}}, m_b, m_{\tilde{b}}$
Quark off-diagonal masses	m_{Y_t}, m_{Y_b}	m_{Y_t}, m_{Y_b}
Quark proto-Yukawa couplings	Y_t, Y_b	Y_t, Y_b
Lepton link couplings	$\Delta_{\tau_L}, \Delta_{\tau_R}$	$\Delta_{\tau_L}, \Delta_{\tau_R}$
Lepton on-diagonal masses	$m_\tau, m_{\tilde{\tau}}$	$m_\tau, m_{\tilde{\tau}}$
Lepton off-diagonal masses	m_{Y_τ}	
Lepton proto-Yukawa couplings	Y_τ	Y_τ
Dimensionality	25	24

Table 1: Parameters present in each model.

The parameter space is defined by a set of model parameters (see Table 1) and their corresponding scan ranges and priors, all of which are detailed in [11]. To reduce computational expense, all mass-dimension parameters are scanned in units of the decay constant f, which is later fixed by its relation to the Higgs vacuum expectation value.

3.3 Experimental constraints

Experimental constraints used in the scans are as those from our previous work: measurements of Standard Model masses (such as m_t, m_b, m_H, and m_τ), electroweak precision observables (e.g. the oblique parameters S and T and Z decay widths), Higgs signal strengths from gluon-fusion production; as well as additional lepton partner mass bounds from LHC searches (see [10, 11] and

references therein for specific constraints). We do not include flavour constraints because doing so would necessitate a more detailed treatment of the flavour structure. Furthermore, we restrict our analysis to partial compositeness of only the third generation, as incorporating the full flavour structure would greatly complicate obtaining a convergent global fit over the complete parameter space. In addition, steep one-sided Gaussian likelihoods are applied to enforce lower bounds on the masses of fermion partners. Multiple scans (each using 4000 live points) were performed and subsequently merged using `anesthetic` [15] to ensure robustness and transparency in our results.

4. Results

For the sake of brevity, we will mainly discuss the results in the context of their Bayesian statistics and key phenomenological results, A full explanation of these results, which include the main scans, detailed analysis and discussion can be found in our original paper [11].

4.1 Model statistics

Model	$\ln(\mathcal{Z})$	$\langle\ln(\mathcal{L})\rangle_P$	$\max\ln(\mathcal{L})$	D_{KL}
LM4DCHM$^{5-5-5}_{5-5}$	-45.60 ± 0.06	-17.27	-10.79	28.33
LM4DCHM$^{5-5-5}_{14-10}$	-36.30 ± 0.05	-14.63	-9.13	21.67

Table 2: Statistics from the combined Bayesian scans of each model, using the priors from **??**.

In Table 2, we present the log-evidence $\ln(\mathcal{Z})$, the posterior-averaged log-likelihood $\langle\ln(\mathcal{L})\rangle_P$, the maximum log-likelihood $\max\ln(\mathcal{L})$, and the Kullback-Leibler divergence D_{KL} of both models. Albeit both satisfy all imposed constraints per Section 3.3 at the 3σ level, the LM4DCHM$^{5-5-5}_{14-10}$ shows an evidence that is four orders of magnitude larger than that of the LM4DCHM$^{5-5-5}_{5-5}$. This decisive preference arises mainly because the LM4DCHM$^{5-5-5}_{14-10}$ has both a higher average log-likelihood and, more importantly, a lower KL divergence, indicating less fine-tuning.

Constraining our priors as in has artificially enhanced the Bayesian evidences, since we deliberately chose these bounds to focus on regions with better likelihoods thus reducing the computational cost of the scans. To further assess prior dependence, we post-processed our samples assuming uniform priors and, separately, using much wider bounds. In both cases, the LM4DCHM$^{5-5-5}_{14-10}$ remains strongly preferred. The large disparity in evidences is primarily driven by the greater fine-tuning required in the LM4DCHM$^{5-5-5}_{5-5}$.

4.2 Experimental signatures

As a result of these scans, we can examine the predicted phenomenology for parameter points in both models that have simultaneously satisfied all constraints and collider bounds at the 3σ level, including the recent quark resonance bounds of 1.54 and 1.56 TeV for the top and bottom partners, respectively [16, 17].

Each model features several heavy quark and lepton partners that could be observed at the LHC, particularly given the predicted sensitivity of the HL-LHC with an integrated luminosity of 3000

fb^{-1}. However, direct detection of these heavy resonances—typically of $O(\text{TeV})$—is generally unfeasible, even for the more promising $\text{LM4DCHM}^{5-5-5}_{14-10}$ model, as shown in Figure 1.

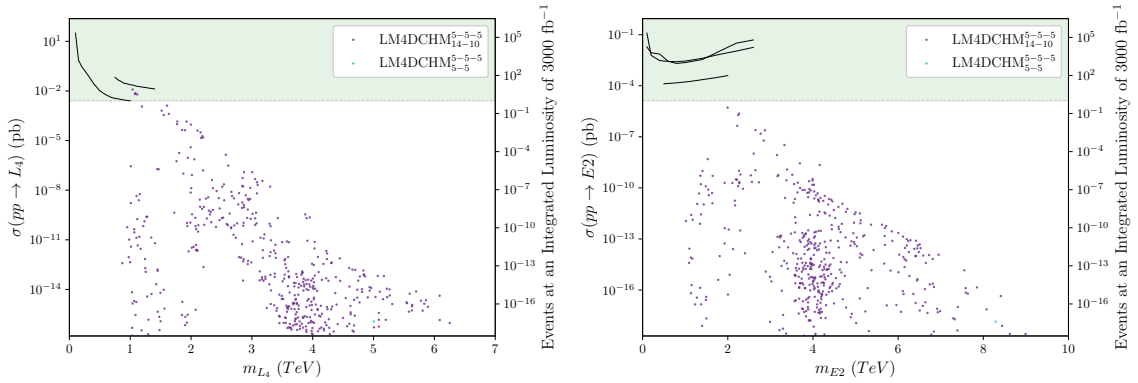

Figure 1: Cross sections for the process $pp \to W/Z \to X$ at $\sqrt{s} = 13$ TeV, where $X = \{L_4, E2\}$ are lightest composite partners with electric charge $\{\mp 1, \mp 2\}$ for valid points in both models. The axis on the right shows the expected number of X particles produced at an integrated luminosity of 3000 fb^{-1} as expected of HL-LHC. The green shaded region is that where the expected number of particles is ≥ 1. Black lines indicate bounds placed by collider search constraints.

Nevertheless, precision Higgs measurements remain excellent tests of these models. In our scenario, the gluon-fusion Higgs signal strengths,

$$\mu^{gg}_{jj} := \frac{[\sigma(gg \to H)\,\text{BR}(H \to JJ)]_{\text{measured}}}{[\sigma(gg \to H)\,\text{BR}(H \to JJ)]_{\text{SM}}},$$

are highly sensitive to modifications in the Higgs couplings to SM gauge bosons and fermions, as well as to loop contributions from composite resonances. Since the predicted signal strengths for both models agree well with the SM value and experimental data (see Figure 2), the prospects for precision measurements of these signal strengths present promising opportunities to test these models in future work—in particular, to assess the viability of the $\text{LM4DCHM}^{5-5-5}_{5-5}$ model.

5. Conclusion

We have obtained convergent global fits of lepton-inclusive MCHMs, finding that both models featuring leptons in different representations can satisfy all imposed experimental constraints. From a Bayesian perspective, the $\text{LM4DCHM}^{5-5-5}_{14-10}$ is definitively more preferred as its evidence is several orders of magnitude greater than that of the $\text{LM4DCHM}^{5-5-5}_{5-5}$, with results that are robust against our choice of priors.

The phenomenology of these models was also analysed, with predicted partners being generally too heavy to be seen, even at the HL-LHC. On the other hand, predictions for gluon-fusion Higgs signal strengths for both models generally align well with experimental bounds, serving as a promising avenue to indirectly test these models.

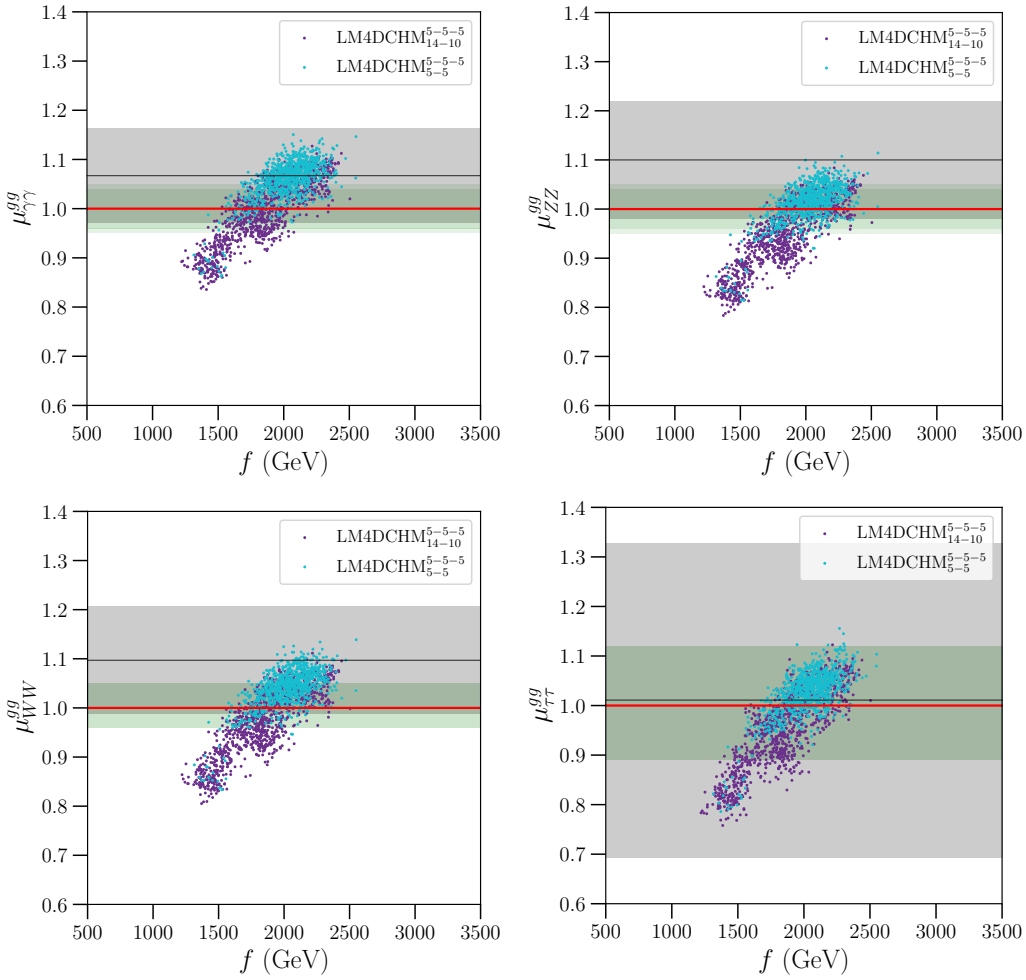

Figure 2: Higgs signal strengths for valid points in both the LM4DCHM$^{5-5-5}_{5-5}$ and LM4DCHM$^{5-5-5}_{14-10}$. Red lines show SM predictions for each decay channel, and the black lines and grey shaded areas show the experimentally measured values and their 1σ uncertainties. Green shaded areas show the projected precision of measurements from the HL-LHC at 3000 fb^{-1}, assuming measurements centred on the SM value of 1.

References

[1] D. B. Kaplan and H. Georgi, $SU(2) \times U(1)$ *breaking by vacuum misalignment*, *Physics Letters B* **136** (1984) 183–186.

[2] D. B. Kaplan, H. Georgi and S. Dimopoulos, *Composite Higgs scalars*, *Physics Letters B* **136** (1984) 187–190.

[3] M. J. Dugan, H. Georgi and D. B. Kaplan, *Anatomy of a composite Higgs model*, *Nuclear Physics B* **254** (1985) 299–326.

[4] R. Contino, Y. Nomura and A. Pomarol, *Higgs as a holographic pseudo-Goldstone boson*, *Nuclear Physics* **B671** (2003) 148–174, [hep-ph/0306259].

[5] K. Agashe, R. Contino and A. Pomarol, *The Minimal composite Higgs model*, *Nuclear Physics* **B719** (2005) 165–187, [hep-ph/0412089].

[6] D. B. Kaplan, *Flavor at SSC energies: a new mechanism for dynamically generated fermion masses*, *Nuclear Physics B* **365** (1991) 259–278.

[7] G. Panico, M. Redi, A. Tesi and A. Wulzer, *On the Tuning and the Mass of the Composite Higgs*, *Journal of High Energy Physics* **03** (2013) 051, [1210.7114].

[8] O. Matsedonskyi, G. Panico and A. Wulzer, *Light Top Partners for a Light Composite Higgs*, *Journal of High Energy Physics* **01** (2013) 164, [1204.6333].

[9] M. Carena, L. Da Rold and E. Pontón, *Minimal Composite Higgs Models at the LHC*, *Journal of High Energy Physics* **06** (2014) 159, [1402.2987].

[10] E. Carragher, W. Handley, D. Murnane, P. Stangl, W. Su, M. White et al., *Convergent bayesian global fits of 4d composite higgs models*, *Journal of High Energy Physics* **2021** (May, 2021) 237.

[11] E. Carragher, K. Goh, W. Su, M. White and A. G. Williams, *Extending global fits of 4D Composite Higgs Models with partially composite leptons*, *JHEP* **08** (2024) 185, [2312.06027].

[12] A. Carmona and F. Goertz, *A naturally light Higgs without light top partners*, *Journal of High Energy Physics* **05** (2015) 1–63.

[13] W. J. Handley, M. P. Hobson and A. N. Lasenby, *PolyChord: next-generation nested sampling*, *Monthly Notices of the Royal Astronomical Society* **453** (2015) 4385–4399.

[14] W. Handley, M. Hobson and A. Lasenby, *PolyChord: nested sampling for cosmology*, *Monthly Notices of the Royal Astronomical Society* **450** (2015) L61–L65, [1502.01856].

[15] W. Handley, *anesthetic: nested sampling visualisation*, *The Journal of Open Source Software* **4** (Jun, 2019) 1414.

[16] ATLAS collaboration, M. Aaboud et al., *Combination of the searches for pair-produced vector-like partners of the third-generation quarks at $\sqrt{s}$ = 13 TeV with the ATLAS detector*, *Phys. Rev. Lett.* **121** (2018) 211801, [1808.02343].

[17] CMS collaboration, A. Tumasyan et al., *Search for pair production of vector-like quarks in leptonic final states in proton-proton collisions at $\sqrt{s}$ = 13 TeV*, *JHEP* **07** (2023) 020, [2209.07327].

PoS(QCHSC24)238